

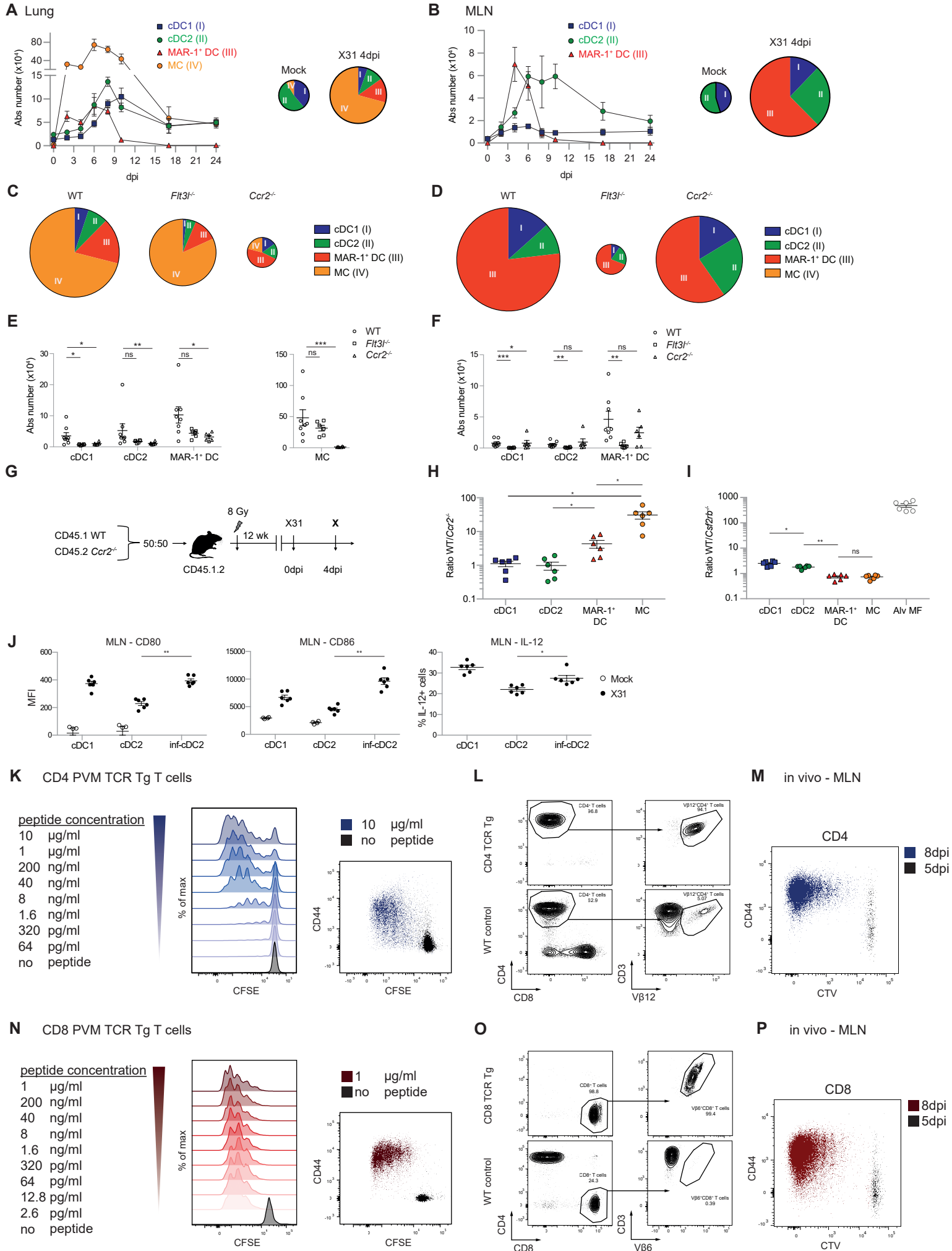
Immunity, Volume 52

Supplemental Information

**Inflammatory Type 2 cDCs Acquire Features
of cDC1s and Macrophages to Orchestrate
Immunity to Respiratory Virus Infection**

Cedric Bosteels, Katrijn Neyt, Manon Vanheerswynghels, Mary J. van Helden, Dorine Sichien, Nincy Debeuf, Sofie De Prijck, Victor Bosteels, Niels Vandamme, Liesbet Martens, Yvan Saeys, Els Louagie, Manon Lesage, David L. Williams, Shiau-Choot Tang, Johannes U. Mayer, Franca Ronchese, Charlotte L. Scott, Hamida Hammad, Martin Guilliams, and Bart N. Lambrecht

Supplementary figure 1



Supplementary Figure 1 (Related to Main Figure 1 & 2) – inf-cDC2s are induced after influenza infection & Functional validation of PVM TCR transgenic mice

(A-B) Kinetics of different lung DC subset (A) and migratory DC subset numbers in MLN (B) upon IAV infection (left panel) and pie charts depicting relative distribution of DC subsets in lung upon mock or 4dpi with IAV (right panel). The size of the pie chart is proportional to the total amount of DCs.

(C-D) Pie charts depicting relative distribution of DC subsets in lung (C) and MLN (D) 4dpi with IAV in WT, *Flt3l*^{-/-} and *Ccr2*^{-/-} mice. The size of the pie chart is proportional to the total amount of DCs.

(E-F) Absolute number of different DC subsets in lung (E) and MLN (D) 4dpi with IAV in WT, *Flt3l*^{-/-} and *Ccr2*^{-/-} mice. Analyzed with a Two-way ANOVA with Sidak correction for multiple comparisons. Error bars indicate ± SEM. *p < 0.05, **p < 0.01, ns = not statistically significant.

(G) Schematic representation of CD45.1 WT: CD45.2 *Ccr2*^{-/-} BM chimeras.

(H) CD45.1/CD45.2 *Ccr2*^{-/-} ratio DC subsets in the lung 4 dpi with IAV. Nine mice were irradiated in two independent rounds and analyzed in 3 different independent experiments. Analyzed with a One-way ANOVA with Sidak correction for multiple comparisons. Error bars indicate ± SEM. *p < 0.05.

(I) CD45.1/CD45.2 *Csf2rb*^{-/-} ratio of DC subsets in the lung 8 dpi with PVM. Eleven mice were irradiated in two independent rounds and analyzed in 2 different independent experiments. Analyzed with a One-way ANOVA with Sidak correction for multiple comparisons. Error bars indicate ± SEM. *p < 0.05, **p < 0.01, ns = not statistically significant.

(J) Expression of CD80 and CD86 shown as MFI and % of IL-12 producing migratory cDCs in the MLN 4dpi with IAV (black dots) compared with mock-infected controls (white dots). For IL-12 staining, samples were restimulated *ex vivo* for 6 hours. Data representative of 2 independent experiments with 3-6 mice per group, analyzed with a One-way (% IL-12+) or Two-way ANOVA (MFI CD80 and CD86) with Sidak correction for multiple comparisons. Error bars indicate ± SEM. *p < 0.05, **p < 0.01.

(K) Histogram showing proliferation as CFSE dilution of CD4⁺ PVM TCR transgenic T cells co-cultured *in vitro* with BMDCs together with exogenous added cognate peptide (M₃₇₋₄₇) in increasing concentrations. Overlay flow cytometry plot (right panel) showing CFSE dilution of CD4⁺ PVM TCR transgenic T cells cultured with BMDCs with 10 µg/ml peptide (blue) or without (black).

(L) CD4⁺ PVM TCR transgenic T cells in peripheral blood of *Rag1*^{-/-} TCR transgenic (upper panel) and WT (lower panel) mouse identified by the expression of the Vβ12 by the TCR.

(M) Congenically marked CD4⁺ PVM TCR transgenic T cells were adoptively transferred i.v. in WT recipients 3dpi with PVM. Overlay flow cytometry plots of the activation and proliferation profile of the exogenous T cells in the MLN 5dpi and 8dpi with PVM.

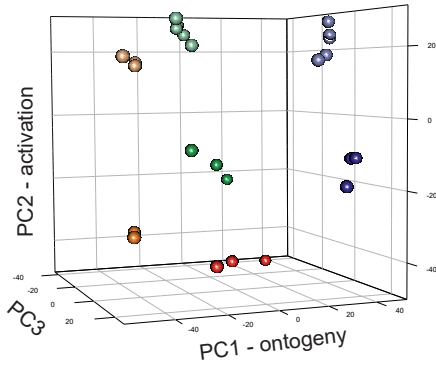
(N) Similar view as in (K) for CD8⁺ PVM TCR transgenic T cells stimulated with N₃₃₉₋₃₄₇ peptide.

(O) Similar as in (L) for CD8⁺ PVM TCR transgenic T cells identified based on expression of Vβ6 by the TCR.

(F) Similar view as in (M) for CD8⁺ PVM TCR transgenic T cells

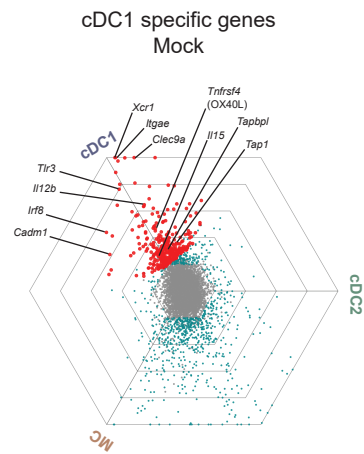
Supplementary figure 2

A



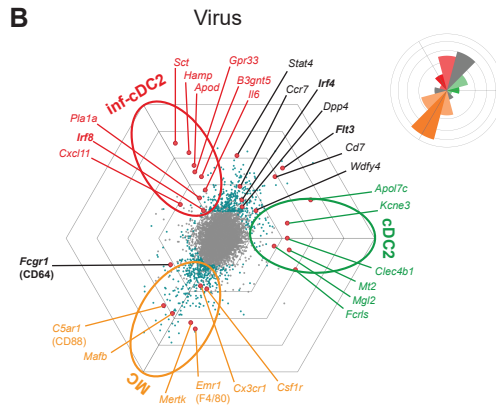
cDC1 mock
cDC1 virus
cDC2 mock
cDC2 virus
MC mock
MC virus

C



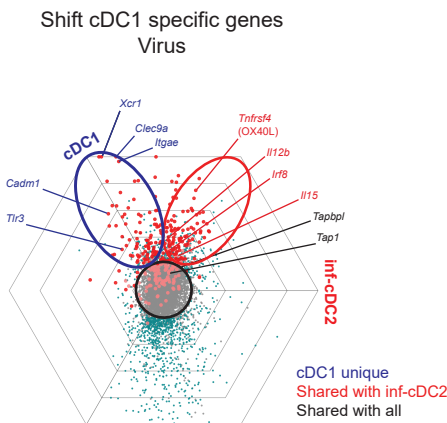
cDC1 specific genes
Mock

B



Virus

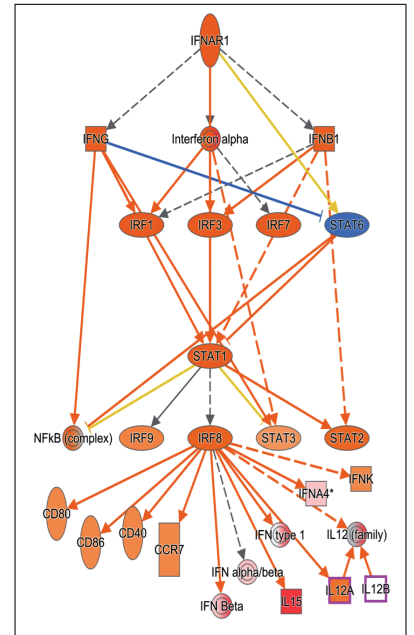
D



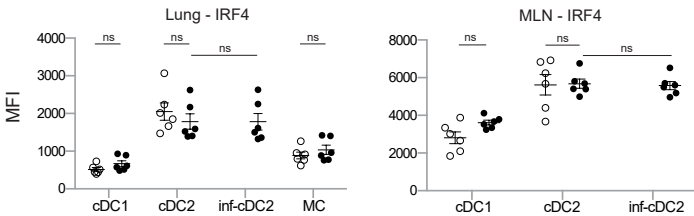
Shift cDC1 specific genes
Virus

cDC1 unique
Shared with inf-cDC2
Shared with all

E



F

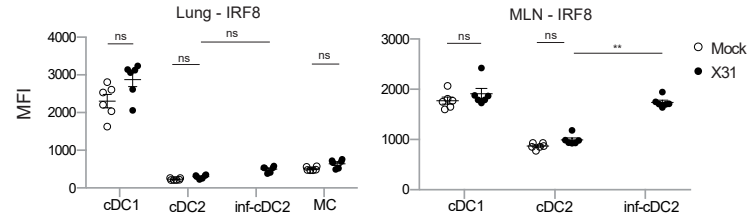


Lung - IRF4

MLN - IRF4

○ Mock
● X31

G

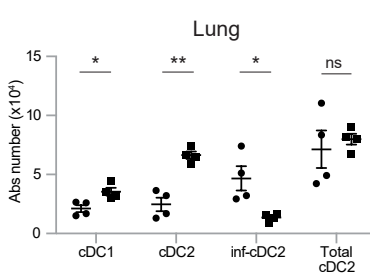


Lung - IRF8

MLN - IRF8

○ Mock
● X31

H

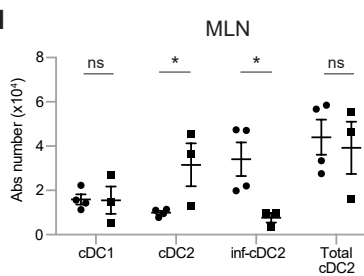


Lung

Lung

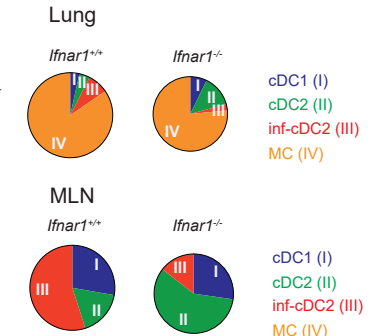
● *Ifnar1*^{+/+}
■ *Ifnar1*^{-/-}

I



MLN

J



Lung

Ifnar1^{+/+}

Ifnar1^{-/-}

cDC1 (I)
cDC2 (II)
inf-cDC2 (III)
MC (IV)

MLN

Ifnar1^{+/+}

Ifnar1^{-/-}

cDC1 (I)
cDC2 (II)
inf-cDC2 (III)
MC (IV)

Supplementary Figure 2 (Related to Main Figure 2, 3 & 4) – Activated inf-cDC2s acquire characteristics of cDC1s

(A) PCA analysis of lung DC subsets 4dpi with mock or IAV.

(B) Triwise diagram highlighting DEG between cDC2s, inf-cDC2s and MCs. Rose diagram (top right corner) shows the percentages of genes in each orientation.

(C-D) Triwise diagram highlighting cDC1 specific genes after mock (C) infection and their shift upon IAV infection (D).

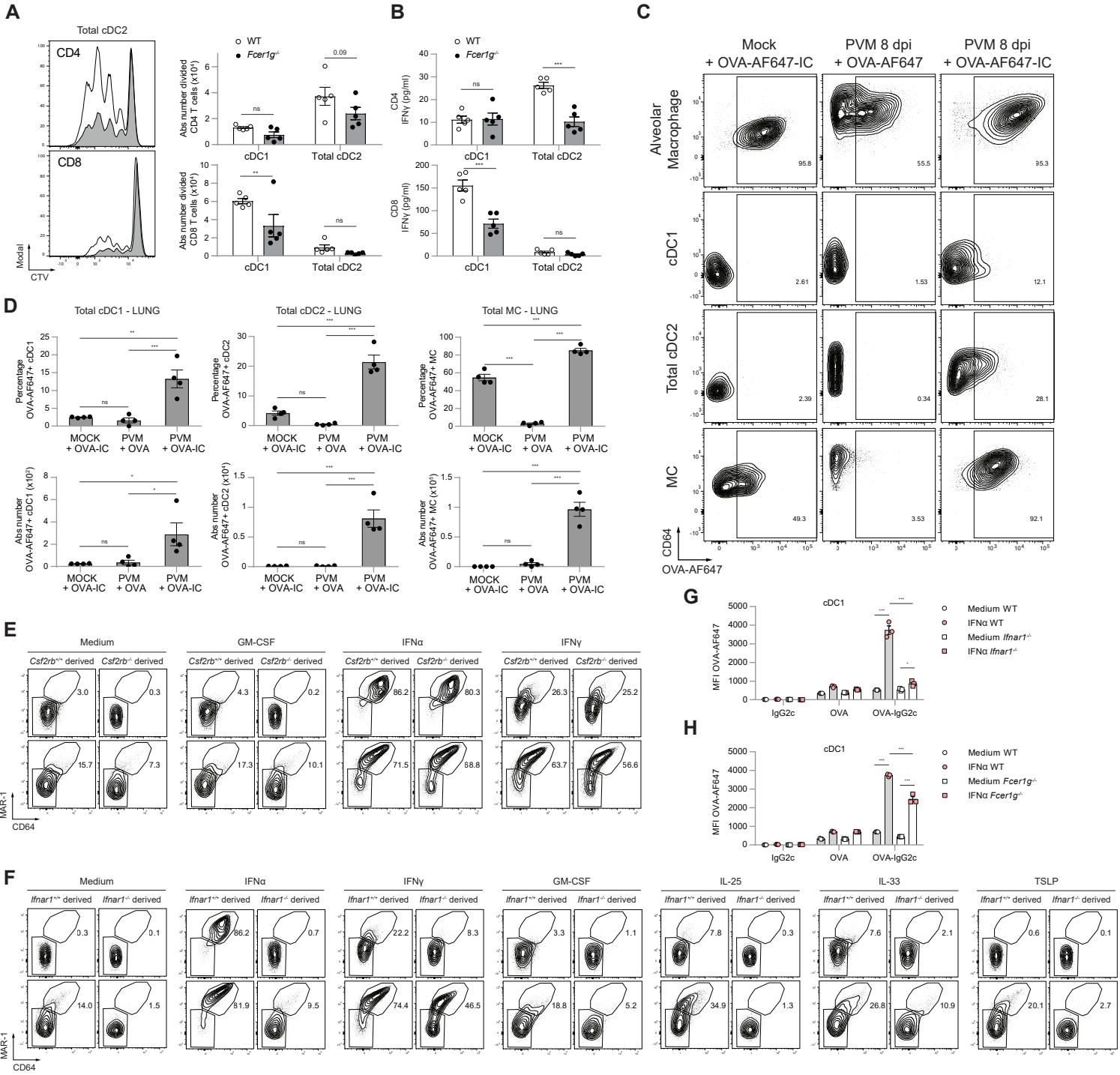
(E) Possible hierarchical clustering of the proposed upstream regulators by IPA regulating the differential gene expression between mock cDC2s and inf-cDC2s.

(F-G) Expression of IRF4 (F) and IRF8 (G) shown as MFI by DC subsets in lung (left panel) and MLN (right panel) 4dpi with IAV (black dots) compared with mock-infected controls (white dots). Data representative of 3 independent experiments with 3-6 mice per group, analyzed with a Two-way ANOVA with Sidak correction for multiple comparisons. Error bars indicate \pm SEM. * $p < 0.05$, ** $p < 0.01$, ns = not statistically significant.

(H-I) Absolute number of DC subsets in lung (H) and MLN (I) of *Ifnar1^{+/+}* and *Ifnar1^{-/-}* mice 4dpi with IAV. Data are representative of 3 independent experiments with 4-5 mice per group, analyzed with a Two-way ANOVA with Sidak correction for multiple comparisons. Error bars indicate \pm SEM. * $p < 0.05$, ** $p < 0.01$, ns = not statistically significant.

(J) Distribution of DC subsets as a % of live DCs in the lung (upper panel) and MLN (lower panel) of *Ifnar1^{+/+}* and *Ifnar1^{-/-}* mice 4dpi with IAV. The size of the pie chart is proportional to the total amount of DCs.

Supplementary figure 3



Supplementary Figure 3 (Related to Main Figure 2 & 4) – Type I IFN dependent FcγR induction licenses cDCs to take up ICs

(A-B) Division of CTV-labeled CD4⁺ and CD8⁺ PVM TCR transgenic T cells cocultured for 4 days with the total cDC2s sorted from 4 pooled MLNs 8dpi with PVM from WT (white) or *Fcer1g*^{-/-} (gray) mice that received PVM immune serum i.t. 6dpi (A). IFN γ measured in supernatans of cocultured CD4⁺ and CD8⁺ PVM TCR transgenic T cells (B). Two-way ANOVA with Sidak correction for multiple comparisons. Error bars indicate \pm SEM. **p < 0.01, ***p < 0.001, ns = not statistically significant.

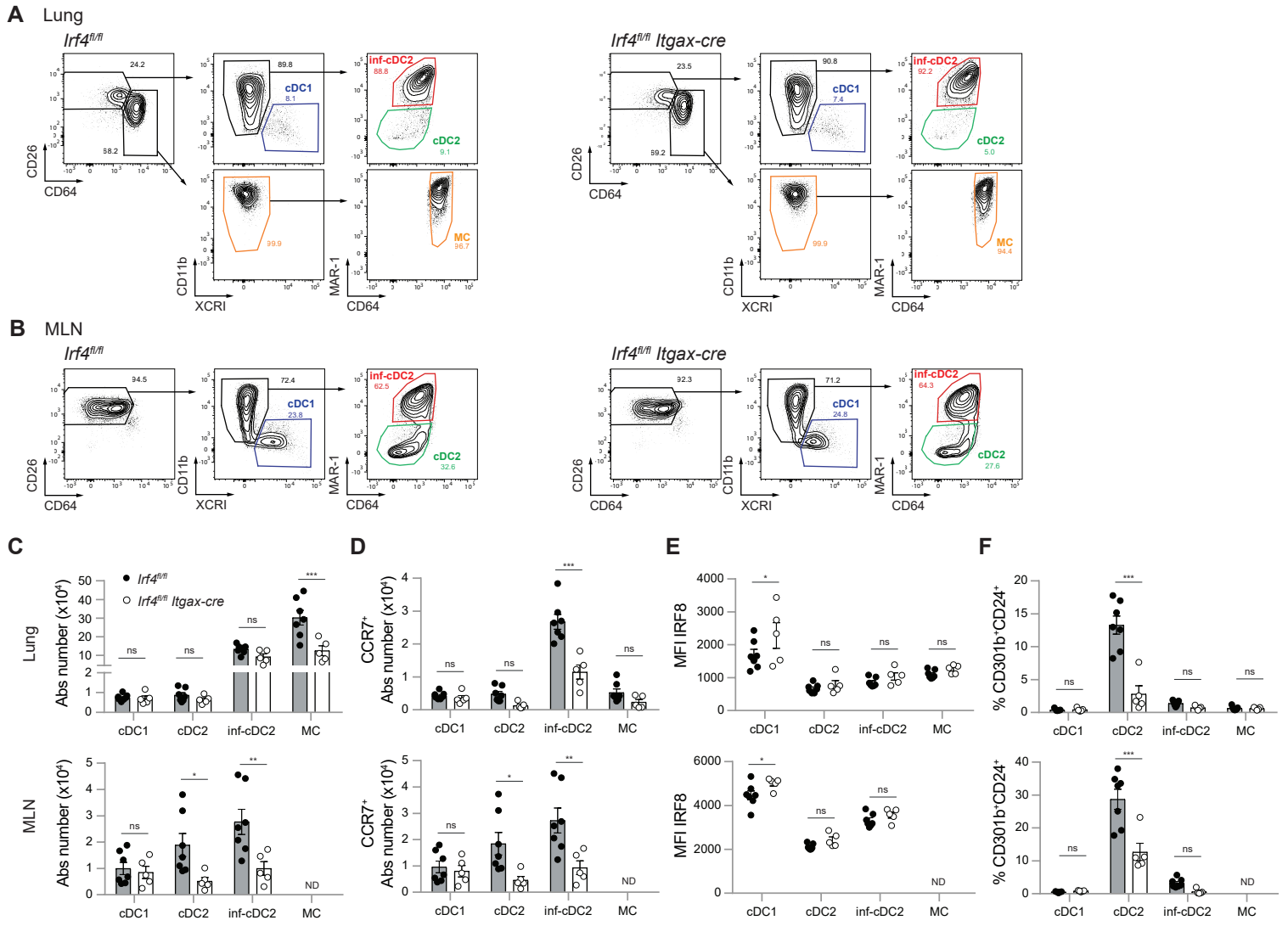
(C) Intracellular CD64 staining and uptake of OVA-AF647 after mock infection or 8dpi with PVM. Mice received 50 μ g OVA-AF647 i.t. either alone or as OVA-AF647-IgG2c-IC at 6dpi.

(D) Percentage (upper row) and absolute number OVA-AF647⁺ DC subsets retrieved from mice as treated in (C). One-way ANOVA with Sidak correction for multiple comparisons. Error bars indicate \pm SEM. *p < 0.05, **p < 0.01, ***p < 0.001, ns = not statistically significant.

(E-F) Flt3L culture of a 50:50 mix of CD45.1 WT and CD45.2 *Csf2rb*^{-/-} (E) or *Ifnar1*^{-/-} (F) DCs stimulated with various cytokines at day 8 and harvested 20h later.

(G-H) Uptake of OVA-AF647 (10 μ g/ml) either added alone or as OVA-AF647-IgG2c-IC 20h after addition to Flt3L culture of a 50:50 mix of CD45.1 WT and CD45.2 *Ifnar1*^{-/-} (G) or *Fcer1g*^{-/-} (H) type 1 cDCs. Data representative of 3 independent experiments with 3 mice per group. Analyzed with a Two-way ANOVA with Sidak correction for multiple comparisons. Error bars indicate \pm SEM. *p < 0.05, ***p < 0.001.

Supplementary figure 4



Supplementary Figure 4 (Related to Main Figure 3) – Lung *Irf4*^{-/-} inf-cDC2s develop normally but have a migratory deficit

(A-B) Gating of DC subsets in lung (A) and MLN (B) of *Irf4*^{fl/fl} (WT) and *Irf4*^{fl/fl} *Itgax-cre* mice 8 dpi with PVM.

(C-D) Absolute number of total (C) and CCR7⁺ (D) DCs in the lung and MLN of *Irf4*^{fl/fl} (WT) and *Irf4*^{fl/fl} *Itgax-cre* mice 8 dpi with PVM.

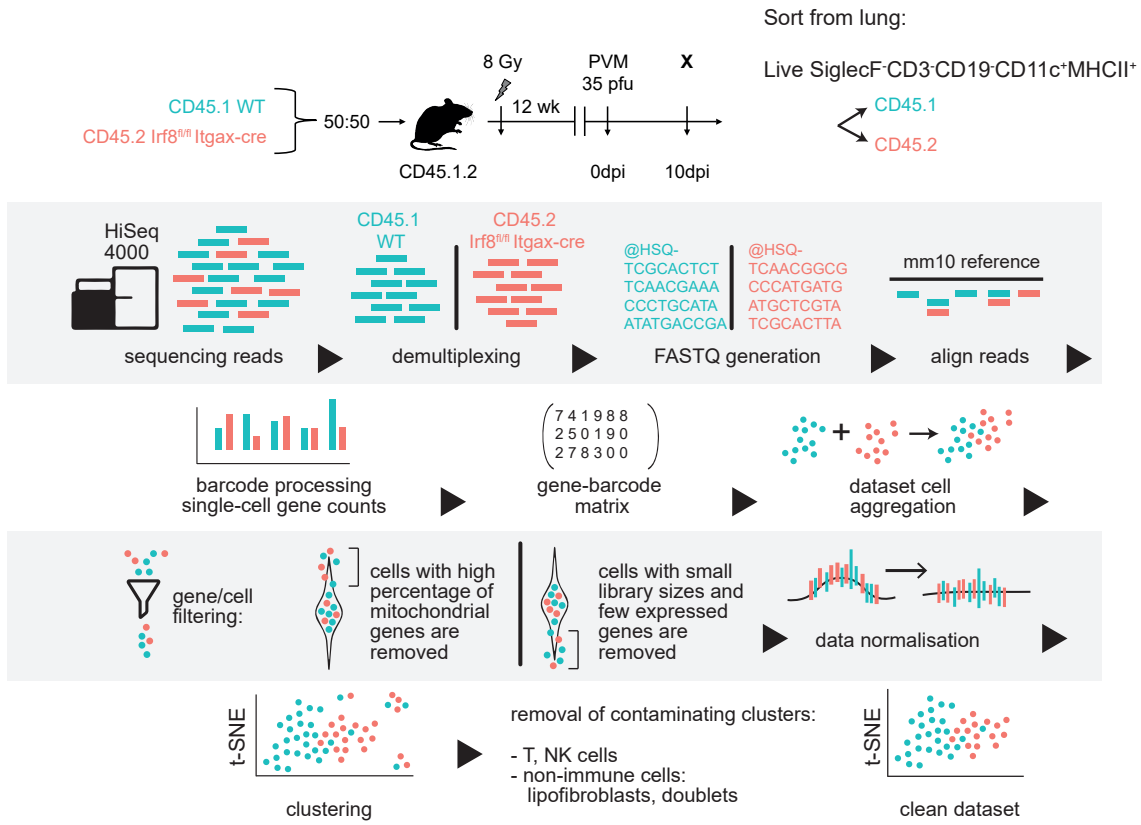
(E) MFI IRF8 by different DC subsets in lung and MLN of *Irf4*^{fl/fl} (WT) and *Irf4*^{fl/fl} *Itgax-cre* mice 8 dpi with PVM.

(F) Percentage of CD301b⁺CD24⁺ DC subsets in lung and MLN of *Irf4*^{fl/fl} (WT) and *Irf4*^{fl/fl} *Itgax-cre* mice 8 dpi with PVM.

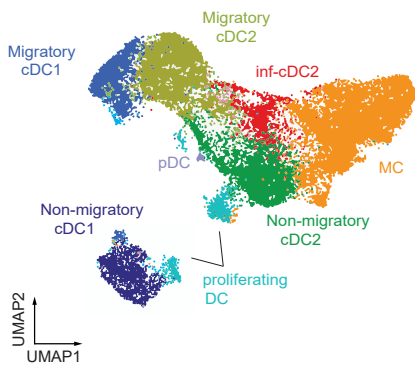
(C-F) Analyzed with a Two-way ANOVA with Sidak correction for multiple comparisons. Error bars indicate \pm SEM. * $p < 0.05$, ** $p < 0.01$, *** $p < 0.001$, .ns = not statistically significant.

Supplementary figure 5

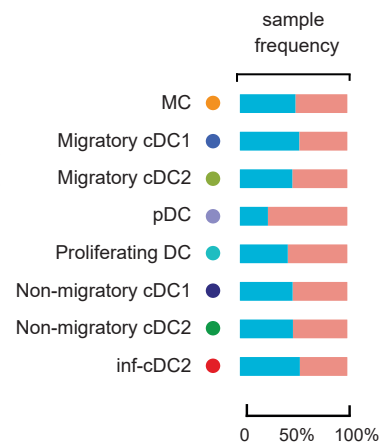
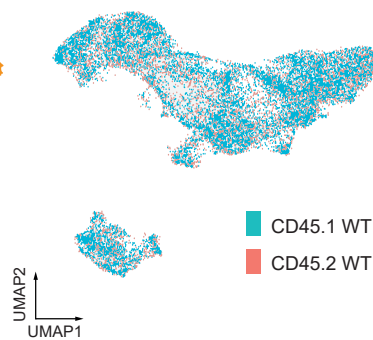
A



B



C



Supplementary Figure 5 (Related to Main Figure 3) – scRNA-Seq pipeline and WT:WT chimeras

(A) Pipeline followed for analysis of scRNA-Seq data.

(B) UMAP plot of SC-RNA-seq data of pooled sorted live CD3-CD19-SiglecF-CD11c+MHCII+ cells from lungs of CD45.1 WT: CD45.2 *Irf8^{fl/fl}* *Itgax-cre^{WT}* chimeric mice 10dpi with PVM, showing assigned clusters.

(C) UMAP plot overlay (left panel) similar to (B) but with the colors representing origin of CD45.1 WT (Teal) or CD45.2 *Irf8^{fl/fl}* *Itgax-cre^{WT}* (Red) compartment and sample frequency per cluster (right panel).